AFRL-AFOSR-VA-TR-2021-0074

The role of the background solar wind on SEP events

Christina Lee
REGENTS OF THE UNIVERSITY OF CALIFORNIA
2150 SHATTUCK AVE RM 313
BERKELEY, CA,
US

07/12/2021
Final Technical Report

Air Force Research Laboratory
Air Force Office of Scientific Research
Arlington, Virginia 22203
Air Force Materiel Command

REPORT DOCUMENTATION PAGE

Form Approved
OMB No. 0704-0188

1. REPORT DATE *(DD-MM-YYYY)*	**2. REPORT TYPE**	**3. DATES COVERED** *(From - To)*
12-07-2021	Final	30 Sep 2016 - 31 Mar 2021

4. TITLE AND SUBTITLE
The role of the background solar wind on SEP events

5a. CONTRACT NUMBER

5b. GRANT NUMBER
FA9550-16-1-0418

5c. PROGRAM ELEMENT NUMBER

6. AUTHOR(S)
Christina Lee

5d. PROJECT NUMBER

5e. TASK NUMBER

5f. WORK UNIT NUMBER

7. PERFORMING ORGANIZATION NAME(S) AND ADDRESS(ES)
REGENTS OF THE UNIVERSITY OF CALIFORNIA
2150 SHATTUCK AVE RM 313
BERKELEY, CA
US

8. PERFORMING ORGANIZATION REPORT NUMBER

9. SPONSORING/MONITORING AGENCY NAME(S) AND ADDRESS(ES)
AF Office of Scientific Research
875 N. Randolph St. Room 3112
Arlington, VA 22203

10. SPONSOR/MONITOR'S ACRONYM(S)
AFRL/AFOSR RTB1

11. SPONSOR/MONITOR'S REPORT NUMBER(S)
AFRL-AFOSR-VA-TR-2021-0074

12. DISTRIBUTION/AVAILABILITY STATEMENT
A Distribution Unlimited: PB Public Release

13. SUPPLEMENTARY NOTES

14. ABSTRACT
During the final reporting period of the research project, the PI and project collaborators developed and tested their methodology towards modeling the transport of solar energetic particles (SEPs) from within the solar corona (< 30 solar radii) to 1 AU in the inner heliosphere. The methodology involves coupling the modeled magnetic fields lines produced from the Wang-Sheeley-Arge solar corona model (WSA; Arge et al., 2003) together with those from the Enlil heliospheric solar wind model (Odstrcil, 2003) and using the SEPMOD code (Luhmann et al., 2007; 2010) to model the transport of SEP protons along those coupled field lines. The task of connecting the WSA field lines to those with Enlil has been non-trivial since the magnetic field line tracing information from WSA (e.g., the position and magnitude of the field line tracing at each step, from 21.5 RâŠ™ down to the solar photosphere at 1 RâŠ™) is not routinely provided as input into Enlil

15. SUBJECT TERMS

16. SECURITY CLASSIFICATION OF:			**17. LIMITATION OF ABSTRACT**	**18. NUMBER OF PAGES**	**19a. NAME OF RESPONSIBLE PERSON**
a. REPORT	**b. ABSTRACT**	**c. THIS PAGE**			JULIE MOSES
U	U	U	UU	11	**19b. TELEPHONE NUMBER** *(Include area code)* 426-9586

AFOSR YIP FA9550-16-1-0418

The role of the background solar wind on SEP events

Christina O. Lee
Space Sciences Laboratory, University of California – Berkeley

Final Report (09/30/2016 – 03/31/2021)

1. Annual Accomplishments: Summary

During the final reporting period of the research project, the PI and project collaborators developed and tested their methodology towards modeling the transport of solar energetic particles (SEPs) from within the solar corona (< 30 solar radii) to 1 AU in the inner heliosphere. The methodology involves coupling the modeled magnetic fields lines produced from the Wang-Sheeley-Arge solar corona model (WSA; Arge et al., 2003) together with those from the Enlil heliospheric solar wind model (Odstrcil, 2003) and using the SEPMOD code (Luhmann et al., 2007; 2010) to model the transport of SEP protons along those coupled field lines. The task of connecting the WSA field lines to those with Enlil has been non-trivial since the magnetic field line tracing information from WSA (e.g., the position and magnitude of the field line tracing at each step, from 21.5 $R_\odot$ down to the solar photosphere at 1 $R_\odot$) is not routinely provided as input into Enlil.

The motivation behind the development of our methodology is as follows: In the current versions of the WSA-Enlil modeling system that are either used for space weather forecasting by NOAA/SWPC or for scientific research at the NASA/CCMC, coronal mass ejection (CME) shocks that form within 21.5 solar radii ($R_\odot$) are not modeled since this coronal region occurs outside the Enlil modeling domain. Meanwhile, within the WSA modeling domain a mathematical description for coronal shocks does not currently exist. It thus follows that the transport of SEPs that are associated with flare or CME shocks that form within 21.5 $R_\odot$, i.e., the highest energy protons that produce ground level enhancement (GLE) events observed at Earth, are currently not modeled by SEPMOD when utilizing the modeled shock information derived from WSA-Enlil.

To test our initial methodology, we use the CME events in September 2017, which produced a very widespread SEP proton event that was detected by multiple spacecraft located across 300° in heliolongitude. The inner heliospheric observers include Earth, STEREO-A along the 1 AU orbit (Kaiser, 2005), and Mars located at ~1.5 AU. During this event, Earth was magnetically well-connected to the solar activity region and therefore detected a ground level enhancement (GLE) event triggered by ~1 GeV SEP protons. Our prior modeling results of this event period (Luhmann et al. 2018; Lee et al., 2018) showed that a portion of the SEP event was not captured because the particle acceleration occurred early on when the CME shock formed within the solar corona, i.e. inside the WSA modeling domain. The SEPMOD results from these earlier runs are used as a baseline for comparison with the new SEPMOD generated the implementation of the coupled WSA-Enlil magnetic field lines. By including the coronal portion of the field lines for the SEP transport, as a first step we are able to model the SEP protons that are mirrored toward the Sun and

reflected back out into the heliosphere by the coronal magnetic fields. These reflected particles contribute to the total particle fluxes observed at 1 AU.

2. SEPMOD Modeling Results for the September 2017 Event Period – Baseline Set

During the first half of September 2017, at least 9 CMEs erupted, some of which impacted Earth. The largest SEP event detected was due to a CME that erupted on 10 September 2017. This event is noteworthy because the SEP protons associated with a fast CME event triggered a ground level enhancement (GLE) event at Earth and also a GLE-like event at Mars (Lee et al., 2018; Luhmann et al., 2018; Zeitlin et al., 2018).

Using the version of WSA-Enlil at the NASA Coordinated Community Modeling Center (CCMC), retrospective fits were made for this event period, with a focus on the observer locations of Earth, STEREO-A and Mars. From the Enlil output, the modeled CME shock parameters, such as the density jump, velocity jump, normal angle to the modeled shock front, and the observer-connected magnetic field line information, such as the field line position (r, theta, phi) and field strength at each position (Br, Btheta, Bphi) were used as input into the SEPMOD code to model the transport of SEPs to all three observer locations. For this project, the focus has been on the Earth observer at 1 AU.

Figure 1 (top panel) shows the lower energy SEP protons measured by EPAM onboard ACE at Earth's L1 and the higher energy protons measured by GOES-13 near Earth. Because Earth was magnetically well-connected to several CMEs during this event period, several SEP proton events were detected, as shown. This includes the GLE event associated with the 10 September 2017 CME event, as labeled near the Day 254 tick mark of this panel. The middle panel shows the

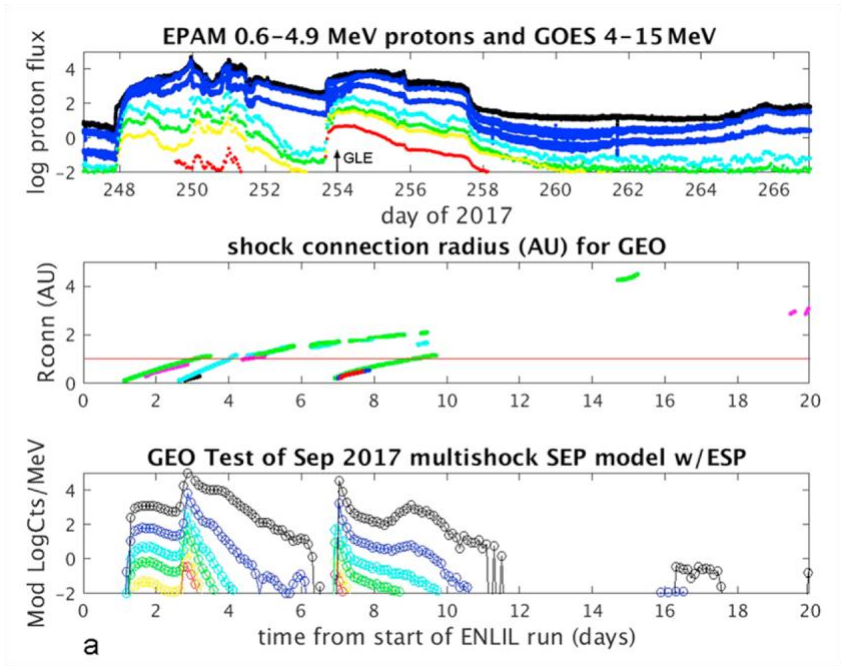

Figure 1. (top panel) Time series of 0.6-4.9 MeV and 4-15 MeV protons observed by ACE/EPAM and GOES during 4-24 September 2017. The x-axis is shown in the day-of-year (DOY) format. (middle panel) Magnetic field line connection of the Earth observer to the modeled CME shocks front as they propagate radially outward from the Sun. The horizontal red line marks the 1 AU radial distance. (bottom panel) Time series of the modeled SEPs by SEPMOD. The x-axis of the two bottom panels shows the start time of the Enlil run (0 = 4 September 2017). Figure from Luhmann et al. (2018).

remote magnetic connection ('Rconn') of the Earth observer to the shock fronts of the modeled cone CMEs in the Enlil simulation. The leftmost green segment (indicating the connection to the 4 September 2017 CME that was launched into the Enlil simulation grid) shows that Earth was magnetically connected to this CME early on in the event, when the CME shock was developed close to the Sun. In this example, the magnetic connection of Earth to this shock front is maintained as the modeled CME propagated just beyond 1 AU (green segment crossing the horizontal red line in the y-axis direction), after which there was no longer a connection to the CME shock.

The bottom panel shows the modeled fluxes of SEP protons with similar energies (i.e., same color coding) as those shown in the top panel. When comparing the modeled proton fluxes with those that were measured by ACE/EPAM and GOES, we see that SEPMOD is able to capture the gross features of the observed fluxes. However, it is noticeable that SEPMOD misses the SEP proton fluxes that occurred near the beginning of the time series (at Day 0 of the bottom panel) and also at the start of the GLE event (near Day 7 of the bottom panel). This is in part due to the CME shocks being formed closer to the Sun (~5-10 $R_\odot$), and therefore are not modeled by Enlil since the inner numerical boundary starts at 21.5 $R_\odot$. As a result, SEPMOD does not capture the SEPs that are accelerated inside the solar coronal region. The SEPMOD results shown in Figure 1 will be used as a baseline set for comparison with the results shown in Section 4 that will utilize connected field lines tracings that start within the WSA modeling domain and out into the Enlil modeling domain.

3. Coupling the WSA Coronal Field Lines with the Enlil Heliospheric Field Lines

The WSA coronal model is composed of the Potential Field Source Surface (PFSS) model, which calculates the field line positions and values from the photosphere at 1 $R_\odot$ out to the source surface distance of 2.5 $R_\odot$, and the Schatten Current Sheet (SCS) model, which calculates the field line positions and values from 2.5 $R_\odot$ out to the outer coronal boundary of 21.5 $R_\odot$. By definition the last closed field line occurs at 2.5 $R_\odot$ and the open field lines that thread through the source surface are radial (i.e., there is no Bphi or Btheta component to the magnetic field). The SCS model is then used to obtain more realistic field line positions and values for the outer solar corona. Synoptic maps of the photospheric magnetic fields are used as input to WSA. For this portion of the research, WSA version 4.5 was used, which provides a user the option of outputting magnetic field line tracings information into a data file. Previously, this

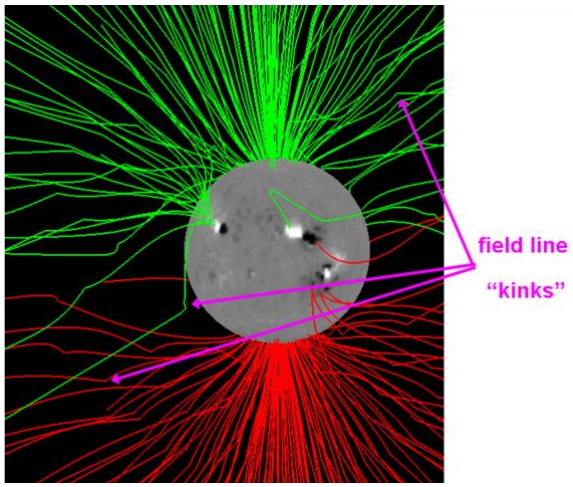

Figure 2. A 3D view of the modeled field lines through the PFSS and SCS regions in WSA for September 4, 2017. The red and green lines denote the negative and positive field polarity. A synoptic map of the photospheric magnetic field is projected as a sphere. Magenta arrows illustrate the field line 'kinks' that arise at the interface between the PFSS and SCS modeling regions of WSA.

output option was unavailable with earlier versions of the WSA code. Given that one of the main research objectives is to model the transport of SEP protons along magnetic field line tracings that start inside the solar coronal region, as a first step we generated specialized modeling output files from one of our previous WSA-Enlil simulations cases, specifically the September 2017 SEP event period, generated at the NASA CCMC. These are non-standard output files are generated independently and separately by the WSA and Enlil codes and contain the 3D field line tracing information for each modeling region (i.e., solar corona and heliosphere).

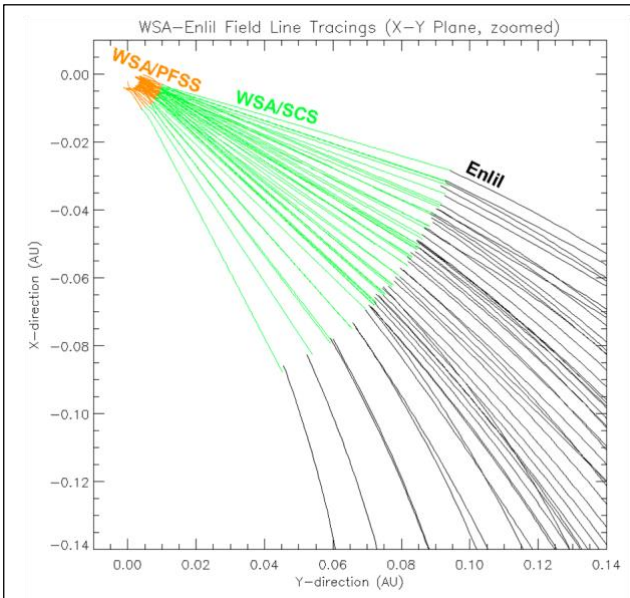

Figure 3. A 2D projection on the X-Y plane of the modeled magnetic field line tracings that connect to an Earth observer at 1 AU. The orange, green, and black lines are derived from the WSA PFSS, WSA SCS, and Enlil modeling regions. As with Figure 2, a discontinuity in the field lines can be seen between the Enlil and WSA at the interface boundary of 21.5 $R_{\odot}$.

Figure 2 shows the field line tracings through the PFSS and SCS regions in WSA, where the red and green lines are negative (toward) and positive (away) polarity fields. Kink-like features can be seen in the magnetic field line tracings, which occur at the source surface height of 2.5 $R_{\odot}$, the location of the interface boundary that separates the WSA PFSS and SCS modeling regions. The kinks are artifacts due to the discontinuous behavior in the magnetic field across the interface boundary between PFSS and SCS. While this does not affect the standard Enlil simulation results (e.g., the WSA-Enlil forecasts at NOAA/SWPC) since the WSA field line position information is not used as input into Enlil, for modeling the transport of SEPs along these field lines, we have to be cautious in using these WSA field line tracings "as is" since the kinks will affect the guiding center motion of SEPs.

Figure 3 shows a zoomed-in, ecliptic plane perspective of a collection of magnetic field line tracings from WSA (orange and green segments from PFSS and SCS modeling regions) and Enlil (black), as labeled. Each Enlil field line tracing shown is connected to the Earth observer (not shown) during the modeled event period of September 4 to 23, 2017 and has an associated event time and date. These tracings start from r = 21.5 $R_{\odot}$ (0.1 AU) out to 258 $R_{\odot}$ (1.2 AU). Essentially, the collection of Enlil field lines shown represents time snapshots of the Earth-connected field lines for modeled event period. Connected to the Enlil segments are those from WSA for the Earth-connected observer. Since the WSA field line tracings are not routinely provided as output into Enlil, additional steps are required for identifying the WSA counterparts of the Enlil Earth-connected field lines. To do so, the first step is to 'align' the numerical grid of WSA to the Enlil grid at the 21.5 $R_{\odot}$ interface. The alignment is non-trivial since the starting grid values of the Enlil longitude is not the same as those for WSA. Also, the spatial resolution is different for the two models. In regard to the starting longitude values, the Enlil longitude grid always starts at 0°, whereas the WSA longitude grid starts at the value of the leading-edge longitude of the input

synoptic photospheric magnetic field map. The values range between 0° to 360° and differs each time depending on the input synoptic maps utilized for the WSA run. In addition, there is an offset applied to the input WSA longitude values by Enlil that takes into account the average amount of time it takes for the nominal solar wind to propagate from the photosphere out to 21.5 $R_{\odot}$.

As an outcome of this part of the project, a numerical routine has been developed to do the following: 1) Retrieve the Enlil Earth-observer field line files, open/read in the field line positions (r, theta, phi) and corresponding vector values (Br, Btheta, Bphi), 2) calculate the event simulation dates and times at each step for each field line, and store this information into a new field line data array, 3) based on Enlil Earth-observer field line dates and times at r = 21.5 $R_{\odot}$, identify the WSA PFSS and WSA SCS field line tracing files that most likely contains coronal counterpart of the Enlil Earth-observer field lines, 4) open/read the WSA SCS file and retrieve the field line with footpoint latitude and longitude values that most closely matches with those from Enlil at the interface boundary, 5) append the WSA SCS field line information in the field line data array generated at step 2, and 6) repeat steps 4 and 5 for the WSA PFSS portion of the field line tracings. The new data file generated from these steps will thus contain the field line information for an Earth observer that traces from 1 AU and all the way back toward the Sun and down to 1 $R_{\odot}$, and contains the corresponding field line position (theta, phi) and their corresponding vector values at each radial step (Br, Btheta, Bphi). For the September 2017 event simulation, the Enlil code generated 4700 Earth observer-connected field line files. As such, the values of the Enlil field line footpoint latitude, longitude and radial position were extracted from each file and stored into a data array along with the field line time and date information. The corresponding WSA SCS and WSA PFSS field line information were retrieved and appended to this data array using the aforementioned numerical routine.

Referring back to Figure 3, a close examination of the field lines at the 21.5 $R_{\odot}$ interface boundary between the WSA SCS and Enlil modeling regions shows a similar discontinuous behavior that was seen at the interface boundary between WSA PFSS and WSA SCS. This discontinuity is in part due to the different spatial resolutions in latitude (theta) and longitude (phi) of the WSA numerical grid versus that of Enlil, which affects the alignment of the model grid points and in turn affect the alignments of the field line footpoints at this interface boundary. For example, an Enlil field line footpoint at the grid location of theta = 75° and phi = 163° could 'land' between two WSA grid locations with positions of theta_m = 74°, phi_m = 162° and theta_n = 76°, phi_n = 164°. In this example, the field line footpoints from either of the two WSA grid locations could be correct. It should be noted though, that while either grid point locations could be used for obtaining the field line tracing at that given radial step, in this example, the vector values (Btheta, Bphi) at this grid point locations could be very different in terms of magnitude and polarity.

To remedy the field line kink artifacts near the two interface boundaries, as a first step we applied a simple averaging to the field line position (r, theta, phi) and field line vector values (Br, Btheta, Bphi) that occur on each side boundary, for a fixed number of model data points. The number of model data points to use for the averaging was determined by trial and error.

Figure 4a shows a 2D projection on the X-Y plane of the kink features in the Earth-connected field lines that appear at the interface boundary between the WSA PFSS and WSA SCS modeling regions (e.g., Figure 2). Note that only the first 100 Earth observer-connected field lines are plotted,

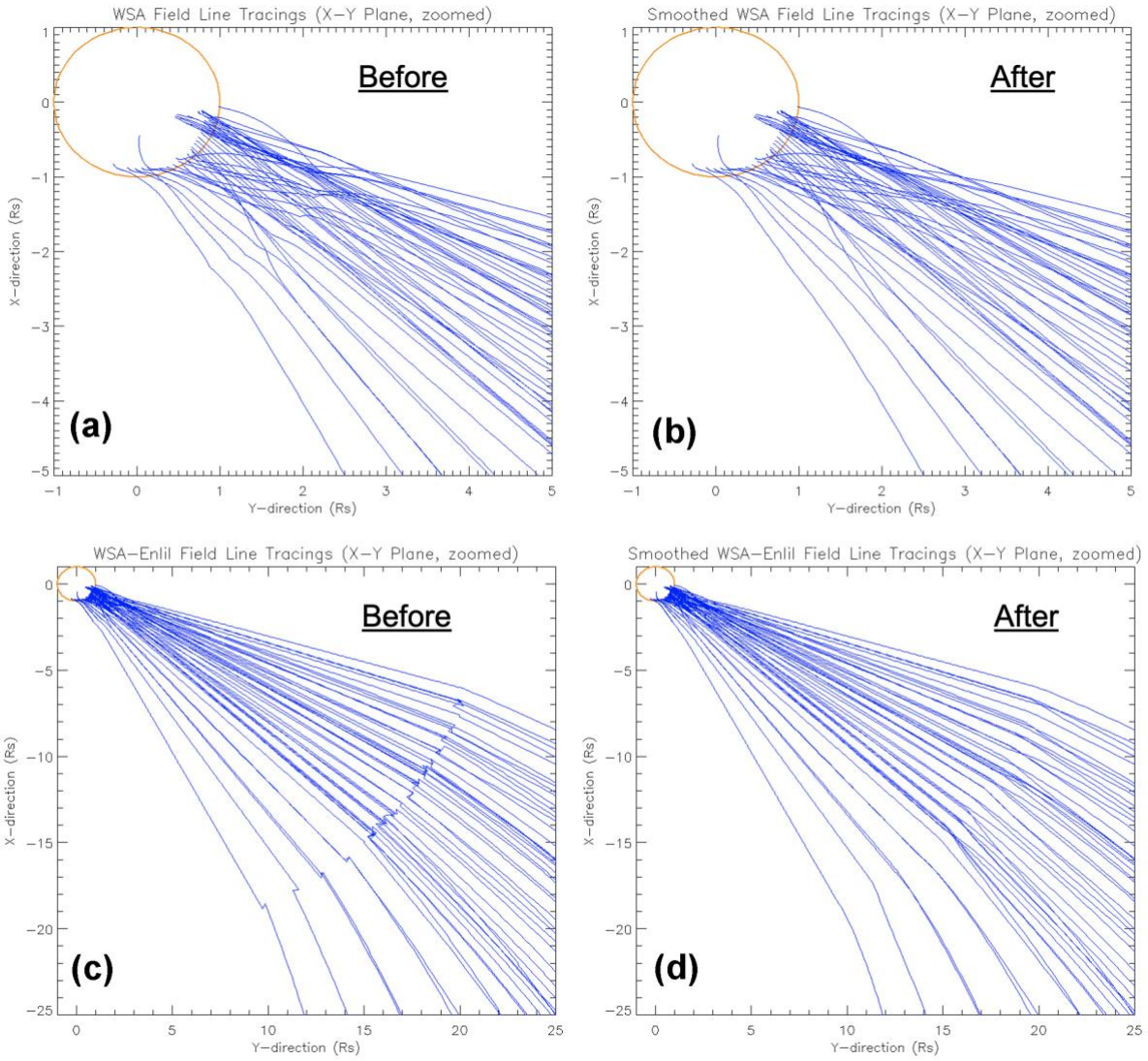

Figure 4. Ecliptic viewpoint of the first 100 magnetic field line tracings from WSA and Enlil. Each field line represents a specific snapshot in time, from 4 to 24 September 2017, of the field line connected from the Sun (orange circle) to the Earth observer at 1 AU (not shown). (a) 'Kinks' at the interface boundary between WSA/PFSS and WSA/SCS modeling regions. (b) The 'kinks' between the WSA/PFSS and WSA/SCS field line segments have been smoothed out and are more continuous. (c) "Kinks' at the interface boundary between the WSA/SCS and Enlil modeling regions. (d) Compared to (c), the "kinks" have been smoothed out and the field line tracings are more continuous at the interface boundary.

out of the 4700 that were generated initially be Enlil. After applying the simple averaging to the field line values for a number of data points 'ahead' and 'behind' this boundary, it can be seen in Figure 4b that the kinks have been smoothed out. Similarly, Figure 4c shows the kink features at the interface boundary between WSA SCS and Enlil modeling regions. In comparison, Figure 4d shows a smoother transition in the field line tracings between these two modeling regions once the simple averaging was applied. In the future, we will refine our averaging methodology by using more sophisticated mathematical techniques.

An outcome of this part of the project is the development of a new piece of numerical code that is easy to use and can be installed and used together with the specialized WSA-Enlil output files that are generated for SEPMOD. This code merges the Enlil heliospheric 'SEP observer' magnetic field lines with those identified from the WSA field line files, smooths the field lines at the interface boundaries of the modeling regions, and generates new output files in a format that is accepted as input by SEPMOD. For SEPMOD to use these new files, a small modification was made in the SEPMOD code to include the additional field line tracing information that extended down to $1R_{\odot}$ from 21.5 $R_{\odot}$.

4. SEPMOD Modeling Results Based on the Coupled WSA-Enlil Field Line Tracings

With the Enlil field lines connected to those from WSA, it is possible to use SEPMOD to model the transport of SEPs accelerated by a shock source that is formed inside the solar corona. Ultimately, our goal is to use WSA-Enlil-cone + SEPMOD to model SEPs accelerated by a moving CME shock that is formed inside the solar corona and a localized shock formed by a solar flare eruption. These SEPs form the population of particles that promptly arrives to an observer that is well-connected to the source region, e.g., a GLE event observed at Earth due to the magnetic connection to the solar west limb flare and/or CME eruption. While a methodology for how to numerically describe a coronal shock in WSA is under development, in the interim, with the connected WSA-Enlil field line tracings we can use SEPMOD to model the SEP protons that get mirrored toward the Sun (by the reverse shock of the CME as it propagates toward the observer) and reflected back out into the heliosphere by the coronal fields.

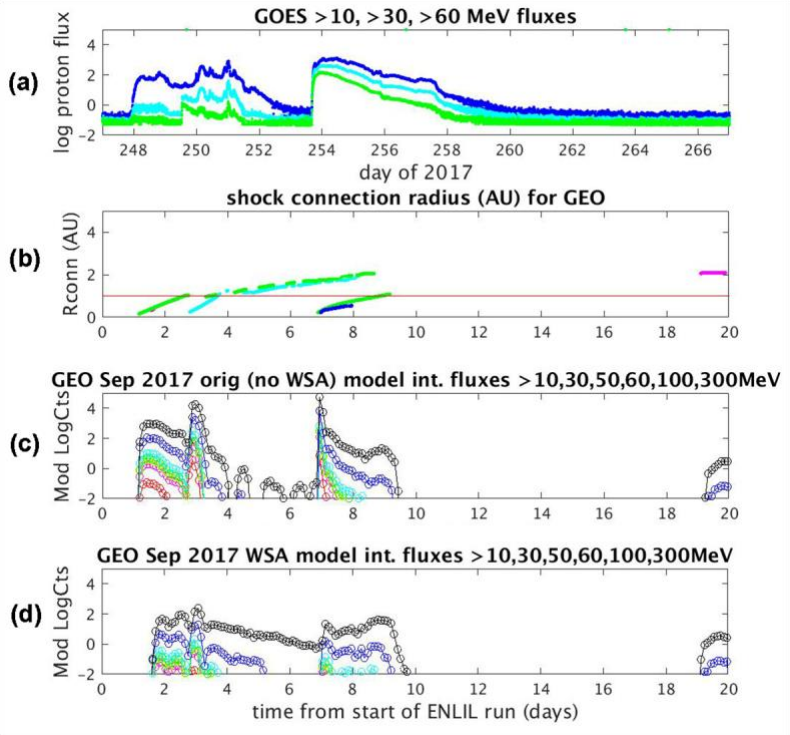

Figure 5. Similar to Figure 1 but with the addition of panel d, which shows SEPMOD proton fluxes that uses the coupled WSA and Enlil field line tracings. The colors shown in c and d represent the proton energies: black = 10 MeV, blue = 30 MeV, green = 50 MeV, orange = 100 MeV and red = 300 MeV. Panel a shows the GOES proton energies at blue = 10 MeV, cyan = 30 MeV, and green = 60 MeV.

Figure 5a to 5c shows the GOES proton fluxes together with the baseline set of SEPMOD results (see Figure 1) together with the new SEPMOD results in Figure 5d that are based on the connected field line tracings from WSA and Enlil. A comparison of Figure 5c with 5d shows that the modeled SEP proton fluxes are different from another. For example, the 10 MeV SEPMOD results (black in Figure 5d) that utilized WSA field line tracings appear to be smoother and more comparable to the GOES observations (blue in Figure 5a), whereas the baseline result for protons at the same energy (black in Figure 5c) shows fluxes that are more prompt (e.g., at Days 3 and 7 in panel c). Qualitatively, the modeled proton fluxes in Figure 5d are more comparable to the GOES integrated fluxes of ~10^3 particles/cm^2/s/sr versus those from the baseline SEPMOD set, where the integrated fluxes are at around ~10^5 particles/cm^2/s/sr or below. Also noticeable in the Figure 5d modeled fluxes of 10 MeV protons (black) and 30 MeV protons (blue) is the additional contribution of fluxes seen from Days 4 through 7 versus the baseline set at the same energies. The contribution of fluxes might be due to the modeled particles that mirrored toward the Sun and subsequently reflected back by the coronal fields in WSA out to the Earth observer. This contribution can also be seen starting at Day 7, where the modeled fluxes show a slight increase in comparison to the baseline set (panel c) and the observed fluxes (panel a).

Future avenues of research will include investigating how the SEPMOD results might improve with modifications to the smoothing algorithm and to the numerical code that identifies the field lines in WSA for connecting to the Enlil Earth observer field lines, as discussed in Section 3. Also, improvements to the fluxes can be made by utilizing the flare particle injection option in SEPMOD, given the addition of the WSA coronal field lines for modeling the transport of SEPs within 21.5 $R_\odot$. Moreover, it will be interesting to also generate a new set of SEPMOD results for the STEREO-A location for this modeled event period. Lastly, in addition to utilizing the September 2017 event as a case study, other SEP events will be used in the future, including those reported in Luhmann et al. (2017) and Luhmann et al. (2018), such as the August 2010, July 2012, and July 2017 SEP event periods.

5. Practical Application Towards Operational Forecasting of SEPs

A prototype version of SEPMOD was recently installed and underwent preliminary testing at the NASA CCMC (see https://ccmc.gsfc.nasa.gov/models/modelinfo.php?model=SEPMOD). A beta version of this code is now available through their Runs-on-Request (RoR) page for users to request SEPMOD results based on specialized WSA-Enlil output results (see https://ccmc.gsfc.nasa.gov/requests/SH/SEPMOD/sepmod.php). As users provide feedback to NASA CCMC on SEPMOD results and as the model matures in its development based on this feedback, there is a potential in the future for SEPMOD to be transitioned and used in support of real-time space weather forecasting operations in support of crewed human missions beyond the low earth orbit (LEO), such as the transit to and operations at the Moon and eventually at Mars. The ability is there to run SEPMOD on real-time WSA-Enlil-cone simulation output, provided that the option in the Enlil code is selected to generate specialized output files for input into SEPMOD, to obtain the SEP event characteristics that are important for forecasting, such as the event onset time, peak fluxes, and event duration (fluence).

The numerical algorithm developed for this project and described in Section 3 provided an opportunity to examine for the first time how the SEPMOD results can be improved when the modeling of SEP protons includes their transport along the coronal magnetic field regions besides the heliospheric field regions. A plan is underway to deliver this algorithm to the NASA CCMC so that users of WSA-Enlil-cone + SEPMOD can have the option to model the transport of SEPs from inside the solar corona out to the heliospheric observer of interest. This plan depends on the further development, testing, and improvements to the existing version of the algorithm, as described in Sections 3 and 4.

If the algorithm is successfully implemented, tested and validated, it will be possible for users of CCMC models to test the capability of WSA-Enlil-cone + SEPMOD + algorithm in realistically simulating the transport of SEP protons for a full event period – and also for a period of multiple SEP events, including the prompt, high-energy particle population. These particles pose as a hazard to human biology and can damage infrastructure and assets in space en route to Moon and Mars and at the surfaces of these beyond-Earth locations. Ultimately, a tested and validated version of SEPMOD with the algorithm developed in this project can hopefully be used together in the future with the operational versions of WSA-Enlil for forecasting SEPs at Earth, Moon, and Mars, in real-time.

6. Programmatic Note: Impact on Research by the COVID-19 Pandemic

The on-going research of this project at the University of California in Berkeley was impacted by the COVID-19 pandemic situation. Starting in mid-March 2020, the PI and project collaborators have been required to work from home (WFH) and have been prohibited from traveling for work locally and out-of-state. The restriction on local work travel caused difficulties for the PI to interact in person and assist in further development, modification, and testing of the SEPMOD code, all of which were necessary this project. The SEPMOD code runs on a local machine in the office of Collaborator J. Luhmann at SSL/UC Berkeley and therefore access to the code was limited and not easily accessible by the PI nor Collaborator Luhmann. Remote access into the machine to use the code was also a challenge. The restriction on out-of-state work travel also impacted the research since this type of travel would have enabled in-person collaborations and research activities that were critical to the success of the project. As a result of this travel restriction, the PI canceled a work trip out to NASA Goddard Space Flight Center, in which the goal was to collaborate in person with Drs. C. N. Arge, D. Odstrcil, and M. L. Mays. For example, on this trip the PI would have obtained, installed, and tested the latest version of the Enlil simulation code onto the project computer and learned how to run the new version of this code. This Enlil version includes an option to more realistically simulate a CME using a spheromak description for the CME cloud, which subsequently could have improved the accuracy of the SEPMOD modeling results of the CME-shock accelerated SEPs. Additionally, the SHINE conference, which was scheduled to take place in July 2020, was also cancelled due to the escalating pandemic situation across the nation at the time. As a result, the PI was unable to present the AFOSR YIP research nor collaborate in person and exchange research ideas with colleagues in the research field (e.g., SEP modelers and colleagues from the space weather forecasting community) who typically attend this annual conference. Lastly, since March 13, 2020 the PI has been providing care to her two young children (ages 5 and 7 years in 2020) due to school closures and cancellations of summer camps, while

working from home. This compounded the problems associated with working from home during the pandemic. This personal situation is ongoing as of June 2021.

7. Publications Resulting from AFOSR YIP Support

The AFOSR Young Investigator Program support has resulted in a number of publications by PI Lee and collaborators. The publications which have already been published in the peer-reviewed literature are as follows:

1. Luhmann, J. G., Mays, M. L., Li, Y., Lee, C. O., Bain, H., Odstrcil, D., Mewaldt, R. A., Cohen, C. M. S., Larson, D., Petrie, G., Shock connectivity and the late cycle 24 solar energetic particle events in July and September 2017, Space Weather, 16(5), 557-568, doi:10.1029/2018SW001860, 2018.

2. Cohen, C. M. S., Luhmann, J. G. Luhmann, Mewaldt, R. A., Mays, M. L., Bain, H. M., Li, Y., Lee, C. O., Searching for Extreme SEP Events with STEREO, 35th International Cosmic Ray Conference (ICRC17), Proceedings of Science, id 301, doi:10.22323/1.301.0134, 2017.

3. Luhmann, J.G., Mays, M. L., Odstrcil, D., Li, Y., Bain, H., Lee, C. O., Galvin, A. G., Mewaldt, R. A., Cohen, C. M. S., Leske, R. A., Larson, D., Futaana, Y., Modeling Solar Energetic Particle Events Using ENLIL Heliospheric Simulations, Space Weather, 15, 934-954, doi:10.1002/2017SW001617, 2017.

Additionally, the majority of the results detailed in this final report, specifically Sections 3 and 4, will be submitted for publication in the near future. It is anticipated that the following paper will be submitted and will acknowledge AFOSR YIP support:

4. Lee, C. O., Luhmann, J. G., Arge, C. N., Odstrcil, D., Mays, M. L., Whitman, K.: Modeling SEP transport from the solar corona out to 1 AU with WSA-Enlil-cone and SEPMOD: A Case Study, *Space Weather*, in preparation, 2021.

REFERNCES

Arge, C.N., Odstrcil, D., Pizzo, V.J., Mayer, L.R.: Improved method for specifying solar wind speed near the Sun. In: Velli, M., Bruno, R., Malara, F., Bucci, B. (eds.) Tenth Internat. Solar Wind Conf. CS-679, AIP, Melville, 190, 2003.

Kaiser, M.: 2005, The STEREO mission: An overview. Adv. Space Res. 36, 1483.

Lee, C.O., Arge, C.N., Odstrcil, D., Millward, G., Pizzo, V., Quinn, J.M., Henney, C.J.: Ensemble Modeling of CME Propagation, *Solar Phys.*, 285, 349-368, 2012.

Lee, C. O., Jakosky, B. M., Luhmann, J. G., Brain, D. A., Mays, M. L., Hassler, D. M., et al., Observations and impacts of the 10 September 2017 solar events at Mars: An overview and synthesis of the initial results, *Geophysical Res. Lett*. (Frontier Article), 45(17), 8871-8885, doi:10.1029/2018GL079162, 2018.

Luhmann, J. G., Ledvina, S. A., Krauss-Varban, D., Odstrcil, D., & Riley, P.: A heliospheric simulation-based approach to SEP source and transport modeling. *Advances in Space Research*, 40(3), 295–303, 2007.

Luhmann, J. G., Ledvina, S. A., Odstrcil, D., Owens, M. J., Zhao, X.-P., Liu, Y., & Riley, P.: Cone model-based SEP event calculations for applications to multipoint observations. *Advances in Space Research*, 46(1), 1–21, 2010.

Luhmann, J.G., Mays, M. L., Odstrcil, D., Li, Y., Bain, H., Lee, C. O., Galvin, A. G., Mewaldt, R. A., Cohen, C. M. S., Leske, R. A., Larson, D., Futaana, Y., Modeling Solar Energetic Particle Events Using ENLIL Heliospheric Simulations, Space Weather, 15, 934-954, doi:10.1002/2017SW001617, 2017.

Luhmann, J. G., Mays, M. L., Li, Y., Lee, C. O., Bain, H., Odstrcil, D., Mewaldt, R. A., Cohen, C. M. S., Larson, D., Petrie, G.: Shock connectivity and the late cycle 24 solar energetic particle events in July and September 2017, Space Weather, 16(5), 557-568, doi:10.1029/2018SW001860, 2018.

Odstrcil, D.: Modeling 3D solar wind structure. *Adv. Space Res*. 32, 497, 2003.

Zeitlin, C., Hassler, D. M., Guo, J., Ehresmann, B., Wimmer-Schweingruber, R. F., Rafkin, S. C. R., et al.: Analysis of the radiation hazard observed by RAD on the surface of Mars during the September 2017 solar particle event, *Geophysical Research Letters*, 45, 5845–5851, doi:10.1029/2018GL077760, 2018.